*Progress In Electromagnetics Research M, Vol. 92, 1–9, 2020*

# The Dependence of Time-Domain Radiation Loss on the Circumference and Wire Radius of a Circular Loop Antenna

**Edmund K. Miller***

**Abstract**—The Lienard-Wiechert potentials show explicitly that charge acceleration, i.e., a change in charge velocity, causes radiation of an electromagnetic field. The goal of this discussion is to explore the rate of energy loss due to radiation from current and charge flowing on a circular loop as a function of the loop's circumference (or curvature) and wire radius. The results presented are obtained using a thin-wire, time-domain (TWTD) computer model for Gaussian-pulse excitation. Some results for a straight wire are also presented for comparison. Representative analytical estimates for the curvature and wire-radius effects are developed from best-fits expressions to the computed results.

## 1. INTRODUCTION

It has been observed [1–5] and quantitatively demonstrated [6] that charge and current (Q/I) waves propagating on a straight wire attenuate or decay with time and distance due to radiation. The amount of similar radiation-caused decay for a circular-loop antenna due to wire curvature and wire radius is explored in the following. Radiation from a straight wire is also included as a reference.

The results presented here are obtained from a well-validated, time-domain, integral-equation model, TWTD (Thin-Wire Time Domain) [7]. A detailed description of the analytical and numerical basis for TWTD can be found elsewhere [8, 9]. Briefly, it is based on a thin-wire approximation to an electric-field integral equation solved using the method of moments. The solution is developed from an explicit time-stepping procedure using a 9-term, second-order polynomial basis expansion in space and time and delta-function sampling.

Modeling an antenna in the time domain usually involves applying an impulsive voltage to one segment of the wire model as is done here. The time-dependent voltage used for the loop results that follow is a Gaussian Pulse as given by

$$V_{ex}(t) = V_o \exp[-a^2(t - t_{mxx})^2]. \tag{1}$$

The loops and dipoles are modeled using a segment length $dx = 0.05\,\mathrm{m}$ long and a time step $dt = 1.667 \times 10^{-10}$ sec so that $cdt = dx$.

Time-domain results are presented below for loop antennas of circumference $C = 2\pi R$ ranging from 5 to 60 m with a wire radius $r$, varying from $10^{-2}$ to $10^{-9}$ m, and for straight wires of comparable length, $L$, and radii. The primary quantity to be examined is an energy measure $W(t)$ [6] derived from their time-dependent propagating current, $I(x,t)$ in amps, and charge density, $Q(x,t)$ in coulombs/m as given by

$$W(t) = \int_0^{CorL} [I^2(x,t) + Q^2(x,t)\, c^2]dx = W_I(t) + W_Q(t) \tag{2}$$

with $c$ the speed of light for free space, and the upper limit of the integral is $C$ for loop circumference, or $L$ for dipole length. The quantities $W_I$ and $W_Q$ are the respective current (or magnetic) and charge

*Received 13 January 2020, Accepted 27 April 2020, Scheduled 9 May 2020*
* Corresponding author: Edmund K. Miller (e.miller@ieee.org).
The author is with the Los Alamos National Laboratory (Retired), USA.

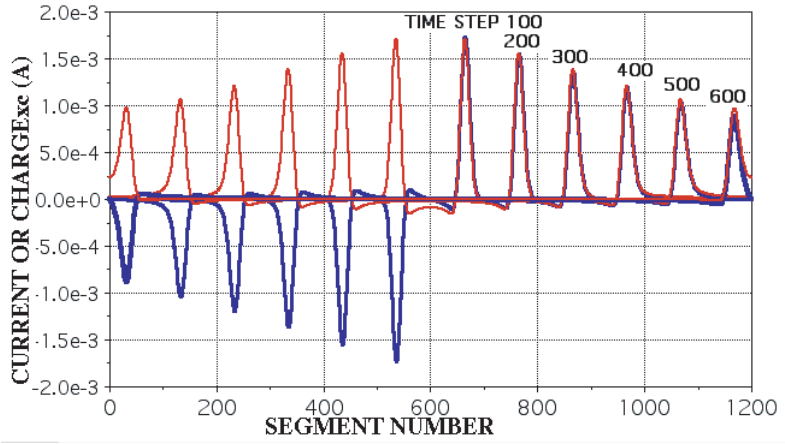


**Figure 1.** The current (red) and charge density times $c$ (blue) on a 1199-segment loop (59.95 m circumference) with a wire radius $r$ of 0.01 m excited at segment 600 by a Gaussian pulse.

(or electric) energies associated with the magnetic and electric fields at the surface of the wire due to the propagating current and charge. Results for the loop and dipole antennas are presented respectively in the following.

A representative example of the impulsive current and charge density for a circular loop having a circumference of 59.95 m (1199 segments) and a wire a radius, $r$, of 0.01 m is shown in Fig. 1 at intervals of 100 time steps. The width parameter, $a$, for the impulsive voltage of Equation (1) is $5 \times 10^{+8}$/sec/ with $t_{\max} = 3 \times 10^{-8}$ sec and $V_o = 1$ V. Note that $I(x,t) = \pm cQ(x,t)$ away the feedpoint at segment 600 or where the counter-propagating charge pulses overlap on the opposite side of the loop. The decay of the current and charge with distance from the feedpoint is clear evidence of the curvature-caused charge acceleration and consequent radiation that occurs.

## 2. NUMERICAL RESULTS FOR THE LOOP ANTENNA

### 2.1. Varying the Loop Circumference

The three energy quantities of Equation (2) are plotted in Fig. 2 for a loop 5-m (100-segments) in circumference with a wire of radius 0.01 m as a function of time step. The width parameter $a = 3.25 \times 10^9$/sec for the variable loop circumferences and radii results that follow. The wide dynamic

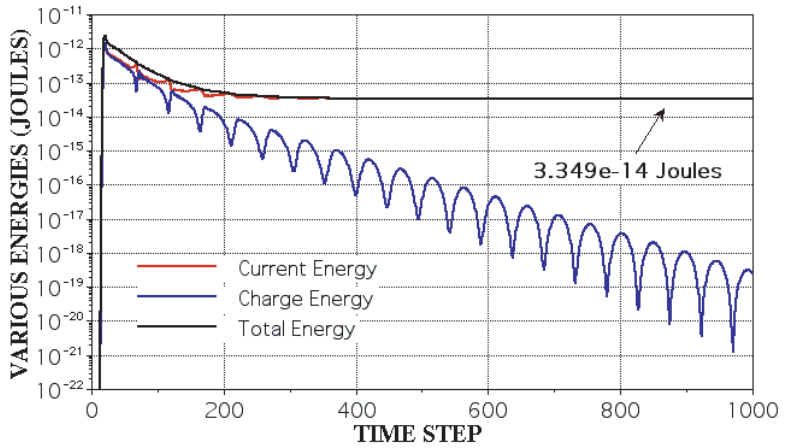


**Figure 2.** The current energy $W_I$, charge energy $W_Q$, and total energy $W$ as a function of time step for a loop of 5 m (100 segment) circumference and wire radius of 0.01 m as a function the time step.

range of this plot is used to demonstrate that $W_Q$ approaches zero with increasing time. The oscillatory decay it exhibits occurs because each time the opposite-signed, oppositely propagating charge pulses meet moving around the loop, they cancel to produce alternating minima. The charge energy eventually becomes zero as the loop radiates the time-dependent energy deposited by the impulsive excitation. This results in a uniform, non-radiating, late-time current $I_o$ and charge neutrality around the loop.

The inductance $L$ of an arbitrary-geometry, Gaussian-Pulse-excited, wire loop is inversely proportional to the late-time current $I_o$ as given by [10, 11]

$$L = \frac{\sqrt{\pi}}{aI_o} = \frac{1.77245}{aI_o} \quad \text{Henries.} \tag{3}$$

Equation (3) yields a value of $4.452 \times 10^{-6}$ Henries with $I_o = 1.225 \times 10^{-4}$ A for the case of Fig. 2. Since the energy stored in an indictor carrying a current $I_o$ is given by

$$W_I = \frac{1}{2} L I_o^2 \,\text{J} \tag{4a}$$

it follows that

$$W_I = \frac{\sqrt{\pi}}{2a} I_o \,\text{J}. \tag{4b}$$

A calibration factor for Fig. 2 is obtained using Equation (4b) of $(1.77245) \times (1.225 \times 10^{-4})/[2 \times 3.25 \times 10^9] = 3.349 \times 10^{-14}$ J.

The time-dependent, normalized total energy on several circular loops of radius 0.01 m and circumferences varying from 5 to 60 m are plotted in Fig. 3(a) and on an expanded scale in Fig. 3(b). A normalized energy is plotted for convenient comparison of the various cases included here, but for this particular example the peak energy is nearly independent of loop size. The decay rates exhibited by the total energy plots in Fig. 3 are initially independent of the loop size. Subsequently they vary not only with loop size but with time as exhibited by the decreasing slopes of the $W(t)$ curves with increasing time. An average decay rate per unit distance for the normalized total energy $W(t)$ to decrease by a $\Delta W$ of 0.2 to 0.1 for the various loop radii of Fig. 3 is plotted on a ln-ln scale in Fig. 4. A best-fit straight line to the data points of Fig. 4 yields a representative analytical estimate for the loop energy-loss rate $\frac{dW_{L,R}(\Delta W,R)}{dx}$ as a function of the loop radius $R$ as

$$Ln\left[\frac{dW_{L,R}\left(\Delta W,R\right)}{dx}\right] = Ln\left[\frac{0.1}{c \times dt\left(TS_{0.2} - TS_{0.1}\right)}\right] \approx -2.7 - 0.77Ln(R). \tag{5a}$$

where "TS$_{xx}$ is the time step at normalized energy level $xx$. On rewriting Equation (5a) in terms of loop circumference $C$ there results

$$\frac{dW_{L,C}\left(\Delta W,C\right)}{dx} \approx \frac{6.72 \times 10^{-2}}{R^{0.77}} = \frac{6.72 \times 10^{-2}}{C^{0.77}} \times (2\pi)^{0.77} = \frac{0.277}{C^{0.77}}. \tag{5b}$$

If instead the average decay rate is estimated using a $\Delta W$ of 0.1 to 0.05 the best-fit straight line in Fig. 4 is given by

$$\frac{dW_{L,C}\left(\Delta W,C\right)}{dx} \approx \frac{2.75 \times 10^{-2}}{R^{0.72}} = \frac{2.75 \times 10^{-2}}{C^{0.72}} \times (2\pi)^{0.72} = \frac{0.103}{C^{0.72}}. \tag{5c}$$

The average $\frac{dW_{L,C}(\Delta W,C)}{dx}$ is found to decrease with increasing loop circumference about as $\sim 1/C^{0.75}$ for which an energy-decrease estimate is given by

$$\frac{dW_{L,C}\left(\Delta W,C\right)}{dx} \approx \frac{K_{L,C}\left(\Delta W\right)}{C^{0.75}} \tag{5d}$$

with $K_{L,C}(\Delta W)$ accounting for the variation in the multiplying constant in Equations (5a) through (5c).

The dependence on loop curvature occurs because the charge acceleration decreases with decreasing loop curvature. The decreasing slope of $W(t)$ with increasing time in Fig. 3 results in $\frac{dW_{L,C}(\Delta W,C)}{dx}$ becoming smaller as the loop currents approach uniformity. Samples of estimated $\frac{dW_{L,C}(\Delta W,C)}{dx}$ values from Equation (5b) and the original samples from Fig. 4 are compared in Fig. 5. They agree within a few percent to validate Equation (5).

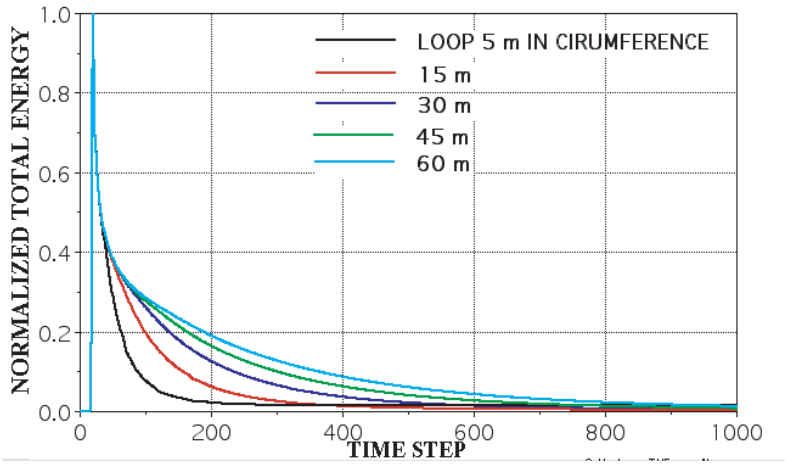


(a)

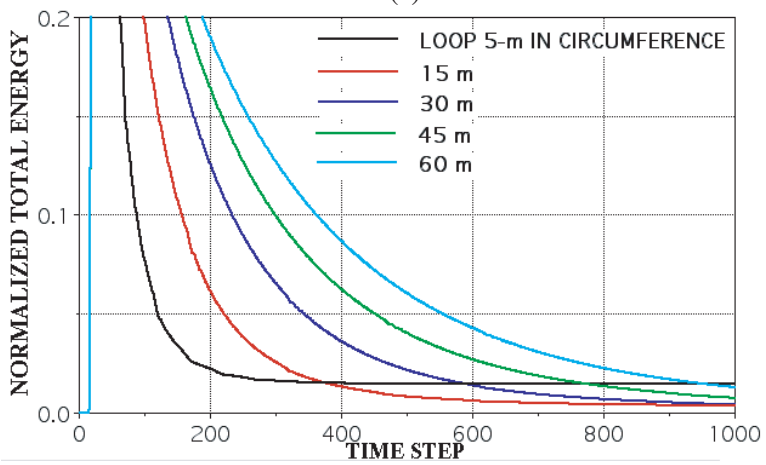


(b)

**Figure 3.** Normalized total energy as a function of time for loops having a wire radius of 0.01 m and variable circumferences in m (a) and on an expanded scale (b).

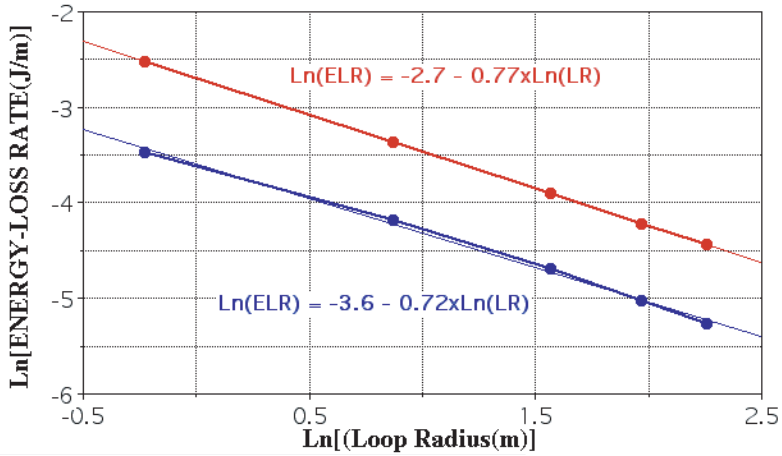


**Figure 4.** The energy-loss rate $\frac{dW_{L,R}(\Delta W,R)}{dx}$ over the normalized ranges 0.2 to 0.1 (red) and 0.1 to 0.05 (blue) as a function of the radius of an impulsively excited circular loop having a wire radius of 0.01 m.

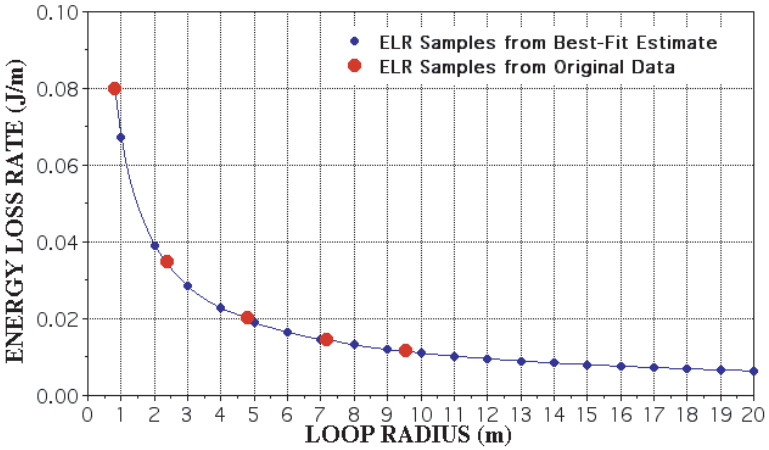


**Figure 5.** The energy-loss rate $\frac{dW_{L,C}(\Delta W,C)}{dx}$ values derived from Figure 3 (the red data points) and samples estimated from Equation (5b) (the blue dots) as a function of the loop radius for a wire radius of 0.01 m.

### 2.2. Varying the Loop Wire Radius

The effect on the normalized energy measure of varying the wire radius for a loop of 5 m (100 segment) circumference is plotted in Fig. 6(a) and on an expanded scale in Fig. 6(b). The energy decay rate is seen to vary with not only the wire radius but also in time as was found above for varying the loop circumference. The average loss rate $\frac{dW_{L,r}(\Delta W,r)}{dx}$ for the results of Fig. 6 was computed over the energy range 0.2 to 0.1 as before. In contrast with the results of Fig. 4, however, plotting the inverse of $\frac{dW_{L,r}(\Delta W,r)}{dx}$ versus $Ln(r)$ now results in a straight-line relationship shown in Fig. 7. A best-fit straight line to the data of Fig. 7 is given by

$$\frac{dW_{L,r}\left(\Delta W,r\right)}{dx}=\frac{0.1}{\left[c\left(TS_{0.2}-TS_{0.1}\right)\right]}\approx\frac{1}{-30+20\mathrm{Log}(r)}. \tag{6}$$

## 3. COMPARING A LOOP AND STRAIGHT WIRE

A comparison of the normalized total energies for loops and straight wires (dipoles) 1199 segments (59.95 m) long and of variable wire radii is presented in Fig. 9. The normalized energy results are numerically identical out to about 180 time steps for $r = 10^{-2}$ m and increasing to about 250 time steps for $r = 10^{-9}$ m. The voltage pulse used for these results has $a = 9.69031 \times 10^{8}$/sec and $t_{\max} = 8.33333 \times 10^{-9}$ sec with $dt = 1.66667 \times 10^{-10}$ sec.

The initial $W(t)$ results here decrease more slowly than those of the 5-m loop of Fig. 6 since the loop curvature in this case is almost 12 times smaller. It can be seen that the dipole and loop have equal normalized energies for 150 or more time steps beyond their peak values. Referring to Fig. 1, the changing shapes (decreasing amplitude and broadening width) with time of the current and charge pulses show that the higher-frequency content is radiated earlier in their propagation along both the loop and dipole. This may explain the early-time equality of their energy loss in Fig. 8.

The normalized energy values at time step 600 are plotted in Fig. 9 as a function of the wire radius for both the loop and dipole. The loop exhibits a greater loss for a given wire radius due to the effect of its curvature.

The $\frac{dW_{D,r}(\Delta W,r)}{dx}$ values averaged over 100 time steps centered at $TS$ 400 for dipoles of various radii whose normalized total energies are obtained from Fig. 9 as given in Table 1 can be estimated using

$$\frac{dW_{D,r}\left(400,r\right)}{dx}\approx\frac{\left[W_{D,r}\left(450\right)-W_{D,r}\left(350\right)\right]}{100} \tag{7}$$

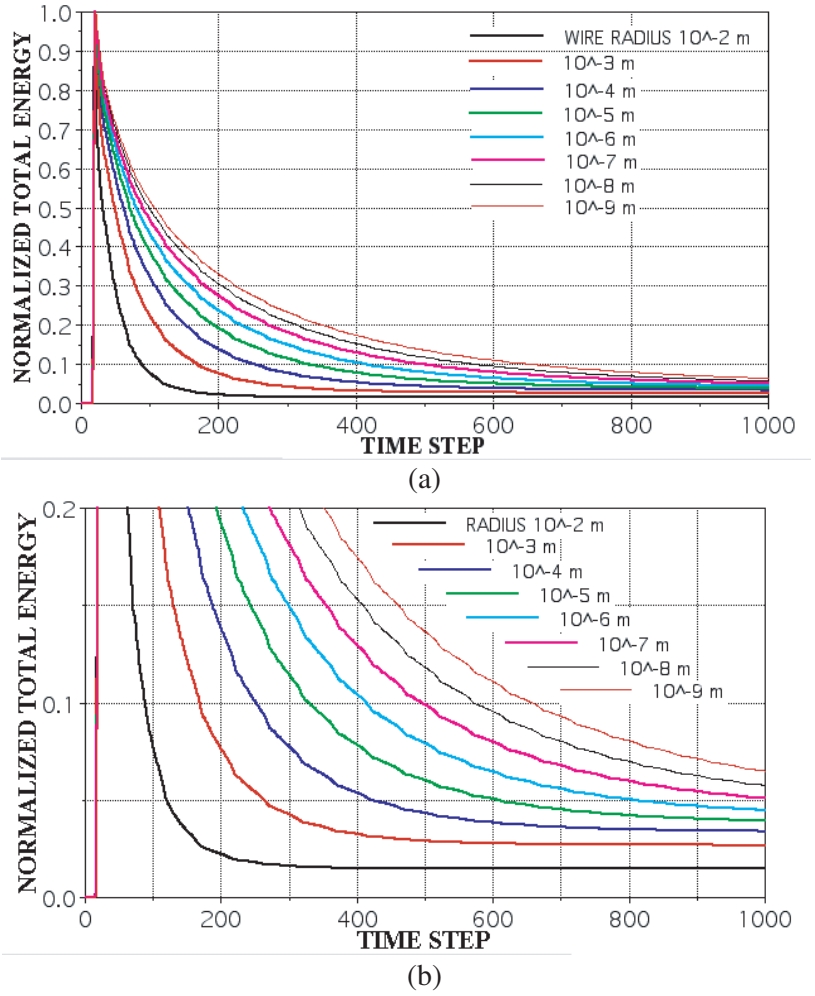


**Figure 6.** Normalized total energy for a loop 5-m (100-segment) in circumference with the wire radius a parameter showing that the loss energy loss rate decreases with decreasing wire radius.

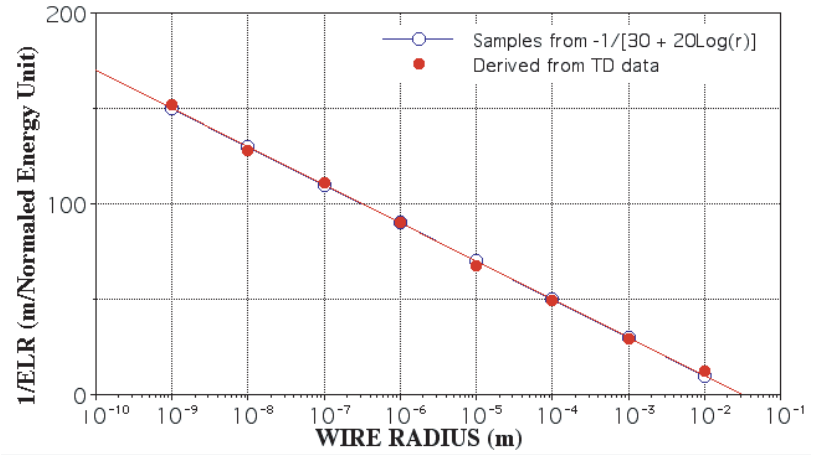


**Figure 7.** The inverse of $\frac{dW_{L,r}(\Delta W,r)}{dx}$ as a function of the radius of a loop 5-m (100 segment) in circumference compared with the model estimate of Equation (6).

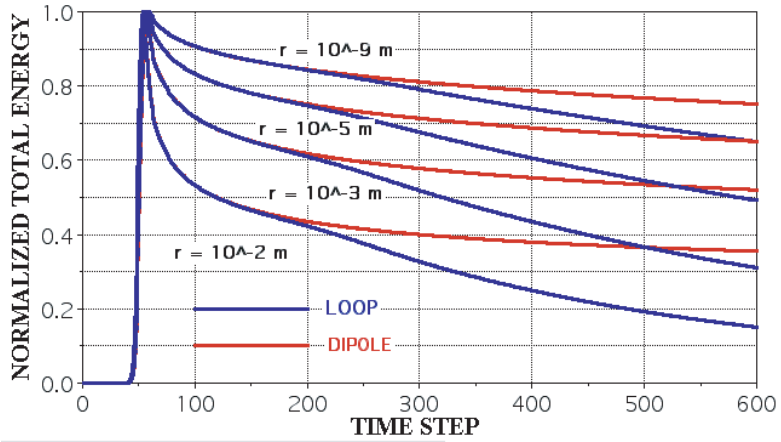


**Figure 8.** The normalized loop energy $W_L(t)$ and dipole energy $W_D(t)$ as a function of time step for several wire radii and total wire lengths of 59.95 m or 1199 segments.

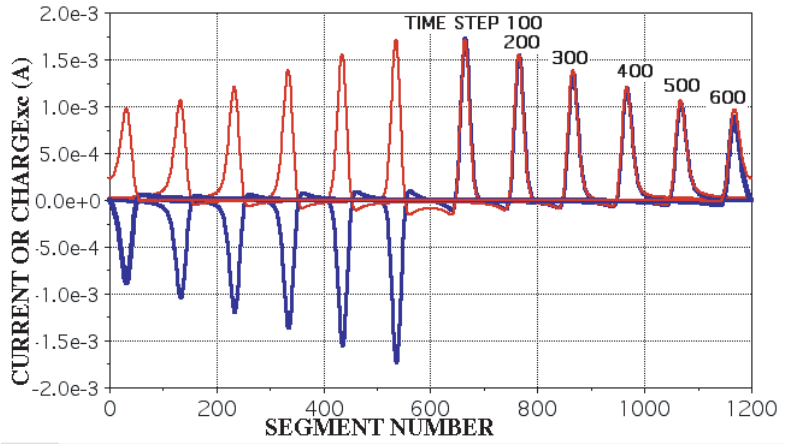


**Figure 9.** The normalized energy at time step 600 as a function of the wire radius for the loop and dipole.

**Table 1.**

| Wire Radius (m) | $W_D$ (350) | $W_D$ (450) | $\frac{dW_{D,r}(400,r)}{dx}$/m |
|---|---|---|---|
| $10^{-2}$ | 0.39 | 0.371 | $1.9 \times 10^{-4}$ |
| $10^{-3}$ | 0.565 | 0.542 | $2.3 \times 10^{-4}$ |
| $10^{-5}$ | 0.7 | 0.678 | $2.2 \times 10^{-4}$ |
| $10^{-9}$ | 0.8 | 0.778 | $2.2 \times 10^{-4}$ |

the results of which shown in Table 1. The average of the four $\frac{dW_{D,r}(400,r)}{dx}$ values in Table 1 is 2.15/m, demonstrating that the late-time energy loss for the dipole is essentially independent of the wire radius over a 7-decade range even though their absolute values differ by a factor of 2 or so.

For comparison, the similarly averaged $\frac{dW_{L,r}(400,r)}{dx}$ values at $TS$ 400 as given by Table 2 show that the late-time energy loss for the 1199-segment loop varies by a factor of about 4/3 over the same range of wire radii. For the 5-m circumference (100-segment) loop of Fig. 6, the $ELR_L$ variation is about 15 to 1.

**Table 2.**

| Wire Radius (m) | $W_L$ (350) | $W_L$ (450) | $\frac{dW_{L,r}(400,r)}{dx}$/m |
|---|---|---|---|
| $10^{-2}$ | 0.285 | .22 | $6.6 \times 10^{-4}$ |
| $10^{-3}$ | 0.475 | .41 | $6.5 \times 10^{-4}$ |
| $10^{-5}$ | 0.6355 | .585 | $5.05 \times 10^{-4}$ |
| $10^{-9}$ | 0.765 | .716 | $4.9 \times 10^{-4}$ |

Samples of the current at successive intervals of 50 time steps on a 1200-segment loop and dipole excited by an impulsive 1-V source at segment 600 are shown in Fig. 10 where $a$ is 9.69 s $10^8$. The pulses are plotted at successive intervals of 50 time steps over the wire half extending from 600 to 1200 segments. Besides the greater decay rate of the loop compared with the dipole, the peak of the loop current is seen to move slightly faster, as a result of the loop's curvature. This is demonstrated in Fig. 11 where best-fit straight lines are fit to the peak space locations as a function of time.

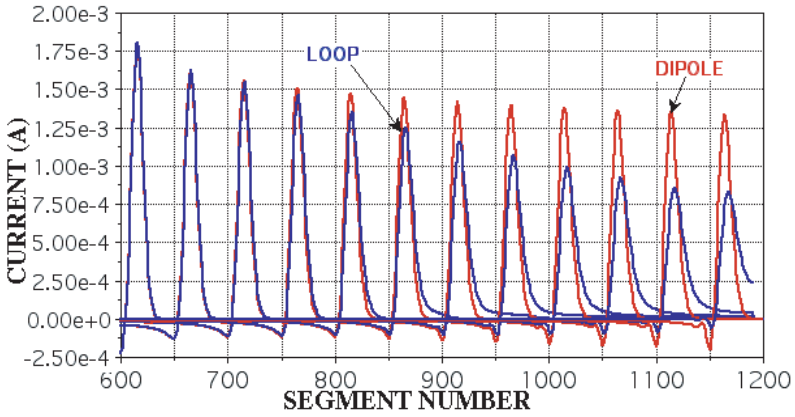


**Figure 10.** The current pulses on 1200-segment (60 m) dipole and circular loop at 50 time-step intervals beginning at time-step 50.

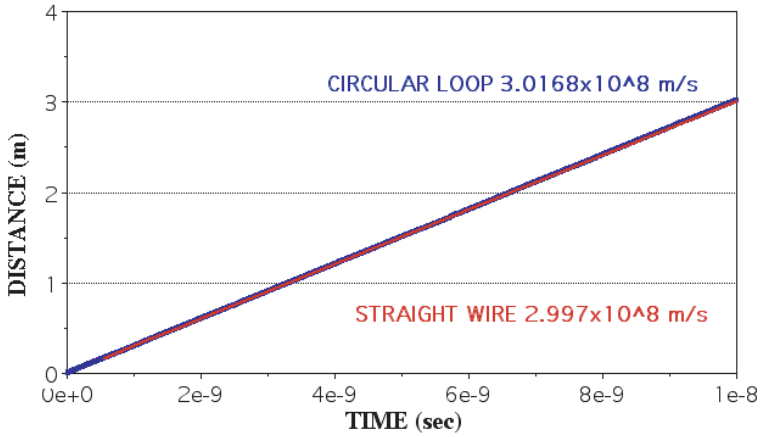


**Figure 11.** Best-fit straight lines to the locations of the peaks of the current pulses of Fig. 10 are shown here as a function of time together with their respective propagation speeds.

## 4. CONCLUDING COMMENTS

Examined above is the influence of the size and wire radius on the rate at which an impulsively excited, circular wire loop loses energy due to radiation. Some results for a straight wire for varying wire radius have been included for comparison. A representative analytical estimate for the energy-decay rate, $\frac{dW_{L,C}(\Delta W,C)}{dx}$, as a function of the loop circumference, $C$, for a wire radius of 0.01 m was obtained as

$$\frac{dW_{L,C}\left(\Delta W,C\right)}{dx} \approx \frac{K_{L,C}\left(\Delta W\right)}{C^{0.75}}. \tag{8}$$

The numerator factor, in Eq. (8), is a variable determined by where in time the decay rate is determined.

Similarly, an estimate of the dependence of the energy-decay rate as a function of the wire radius $r$, $\frac{dW_{L,r}(\Delta W,r)}{dx}$, has been determined from the time-domain results for a 5-m (100-segment) loop to be given by

$$\frac{dW_{L,r}\left(\Delta W,r\right)}{dx} \approx \frac{1}{-30+20Ln(r)}. \tag{9}$$

Observe that Equation (9) was derived specifically for a loop having a wire radius of 0.01 m. Similarly, Equation (10) was developed specifically for a loop 5-m in circumference. The energy-decay rate for the 60-m loop is much less sensitive to the wire radius. Thus, generalizing these results over a wider parameter range, subject to the limits of TWTD, would probably be useful.

## REFERENCES


1. Schelkunoff, S. A., *Advanced Antenna Theory*, John Wiley & Sons, 190, 1952.
2. Jackson, J. D., *Classical Electrodynamics*, John Wiley & Sons, 401, 1962.
3. Shen, L-C., T. T. Wu, and R. W. King, "A simple formula of current in dipole antennas," *IEEE Trans. AP-S*, Vol. 16, No. 5, 542–547, 1968.
4. Anderson, B., "Admittance of infinite and finite cylindrical metallic antenna," *Radio Science*, Vol. 3, No. 6, 607–621, 1968.
5. Jones, D. S., *Methods in Electromagnetic Wave Propagation*, 295, Clarendon Press, 1994.
6. Miller, E. K., "The proportionality between charge acceleration and radiation from a generic wire object," *Progress In Electromagnetics Research*, Vol. 162, 15–29, 2018.
7. Landt, J. A., E. K. Miller, and M. Van Blaricum, "WT-MBA/LLL1B (TWTD): A computer program for the time-domain electromagnetic response of thin-wire structures," Lawrence Livermore Laboratory, Report No. UCRL-51585, 1974.
8. Miller, E. K., A. J. Poggio, and G. J. Burke, "An integro-differential equation technique for the time-domain analysis of thin-wire structures, Part I: The numerical method," *Journal of Computational Physics*, Vol. 12, 24–48, 1973.
9. Poggio, A. J., E. K. Miller, and G. J. Burke, "An integro-differential equation technique for the time-domain analysis of thin-wire structures. Part II: Numerical results," *Journal of Computational Physics*, Vol. 12, 210–233, 1973.
10. Paul, C. R., "Partial Inductance," *IEEE EMC Society Magazine*, 34–42, 2010 (Summer).
11. Miller, E. K., "Time-domain computation of loop inductance," *IEEE EMC Society Magazine*, 34–42, 2011 (Summer).